

# **SANDIA REPORT**

SAND2016-9253

Unlimited Release

Printed September 2016

# **Performance Results for the Prism Solar Installation at the New Mexico Regional Test Center: Field Data from February 15 - August 15, 2016**

Matthew Lave, Joshua S. Stein, Laurie Burnham

Prepared by  
Sandia National Laboratories  
Albuquerque, New Mexico 87185 and Livermore, California 94550

Sandia National Laboratories is a multi-mission laboratory managed and operated by Sandia Corporation, a wholly owned subsidiary of Lockheed Martin Corporation, for the U.S. Department of Energy's National Nuclear Security Administration under contract DE-AC04-94AL85000.

Approved for public release; further dissemination unlimited.



**Sandia National Laboratories**

Issued by Sandia National Laboratories, operated for the United States Department of Energy by Sandia Corporation.

**NOTICE:** This report was prepared as an account of work sponsored by an agency of the United States Government. Neither the United States Government, nor any agency thereof, nor any of their employees, nor any of their contractors, subcontractors, or their employees, make any warranty, express or implied, or assume any legal liability or responsibility for the accuracy, completeness, or usefulness of any information, apparatus, product, or process disclosed, or represent that its use would not infringe privately owned rights. Reference herein to any specific commercial product, process, or service by trade name, trademark, manufacturer, or otherwise, does not necessarily constitute or imply its endorsement, recommendation, or favoring by the United States Government, any agency thereof, or any of their contractors or subcontractors. The views and opinions expressed herein do not necessarily state or reflect those of the United States Government, any agency thereof, or any of their contractors.

Printed in the United States of America. This report has been reproduced directly from the best available copy.

Available to DOE and DOE contractors from  
U.S. Department of Energy  
Office of Scientific and Technical Information  
P.O. Box 62  
Oak Ridge, TN 37831

Telephone: (865) 576-8401  
Facsimile: (865) 576-5728  
E-Mail: [reports@osti.gov](mailto:reports@osti.gov)  
Online ordering: <http://www.osti.gov/scitech>

Available to the public from  
U.S. Department of Commerce  
National Technical Information Service  
5301 Shawnee Rd  
Alexandria, VA 22312

Telephone: (800) 553-6847  
Facsimile: (703) 605-6900  
E-Mail: [orders@ntis.gov](mailto:orders@ntis.gov)  
Online order: <http://www.ntis.gov/search>



# **Performance Results for the Prism Solar Installation at the New Mexico Regional Test Center: Field Data from February 15 - August 15, 2016**

Matthew Lave

Photovoltaic and Distributed Systems Integration  
Sandia National Laboratories  
P.O. Box 969, MS-9052  
Livermore, CA 94551-0969

Joshua S. Stein

Photovoltaics and Distributed Systems Integration  
Sandia National Laboratories  
P.O. Box 5800  
Albuquerque, New Mexico 87185-MS1033

Laurie Burnham

Electric Power Systems Research  
Sandia National Laboratories  
P.O. Box 5800  
Albuquerque, New Mexico 87185-MS1140

## **Abstract**

A 9.6 kW test array of Prism bifacial modules and reference monofacial modules installed in February 2016 at the New Mexico Regional Test Center has produced six months of performance data. The data reveal that the Prism modules are outperforming the monofacial modules, with bifacial gains in energy over the six-month period ranging from 18% to 136%, depending on the orientation and ground albedo. These measured bifacial gains were found to be in good agreement with modeled bifacial gains using equations previously published by Prism. The most dramatic increase in performance was seen among the vertically tilted, west-facing modules, where the bifacial modules produced more than double the energy of monofacial modules and more energy than monofacial modules at any orientation. Because peak energy generation (mid-morning and mid-afternoon) for these bifacial modules may best match load on the electric grid, the west-facing orientation may be more economically desirable than traditional south-facing module orientations (which peak at solar noon).



## CONTENTS

1.	Introduction .....	10
2.	System Design.....	11
2.1.	Module Orientations .....	11
2.2.	Data Acquisition System (DAQ) .....	12
3.	Baseline Testing .....	15
3.1.	Ground Surface Albedo .....	15
3.1.1.	White Ground Surface .....	15
3.1.2.	Natural Ground Surface .....	16
3.2.	Flash Testing.....	16
3.2.1.	Module Front Side Maximum Power .....	16
3.2.2.	I-V Curves .....	18
4.	Performance analysis.....	20
4.1.	Errant and missing measurements .....	20
4.2.	Performance at Various Sun Angles.....	21
4.2.1.	W90 Modules: Solar Angle Dependent Performance .....	21
4.2.2.	All Modules: Solar Time Dependent Performance .....	23
4.3.	Clear vs. Cloudy Conditions .....	25
4.4.	Monthly Bifacial Gains.....	27
4.5.	Energy and Bifacial Gain over Six Month Period .....	29
4.6.	Comparison to Modeled Bifacial Gain .....	30
5.	Conclusions .....	34

## FIGURES

Figure 1: Photograph (top) and schematic (bottom) showing the setup of monofacial and bifacial modules installed at Sandia in Albuquerque, NM. In the schematic, blue represents bifacial modules, red represents monofacial modules, and the two dashed black rectangles indicate the area of crushed white rock that makes up the white ground surface. ....	12
Figure 2: Backside of Prism module showing location of yellow thermocouples. ....	13
Figure 3: POA reference cell (top center of picture) mounted to measure backside irradiance, shown here for one of the monofacial modules in the W90 orientation. Also visible in the lower right is the yellow thermocouple measuring module temperature. ....	14
Figure 4: (Left) Albedometer setup on the white surface. The picture was taken in the afternoon, and shows shading of the ground surface. The picture was taken facing north; the albedometer is east of the W15Wht modules. (Right) Global horizontal irradiance (GHI), ground reflected irradiance (GRI), and albedo as measured by the albedometer. Afternoon shading of the ground and hence reduced GRI is visible, especially on the clear day, and is the reason for the reduced albedo in the later afternoon. ....	15
Figure 5: (Left) Albedometer setup on the natural surface. The yellow line is a tape measure used during installation and was not present during albedo measurements. (Right) Global horizontal irradiance (GHI), ground reflected irradiance (GRI), and albedo as measured by the albedometer. ....	16
Figure 6: Maximum power (Pmp) under STC conditions found from front-side flash testing at Sandia. ....	17
Figure 7: Maximum power (Pmp) under STC conditions found from front-side flash testing at the factory. ....	18
Figure 8: I-V curves for monofacial modules based on flash tests at Sandia. ....	19
Figure 9: I-V curves for bifacial modules based on flash tests at Sandia. ....	19
Figure 10: Data availability for all modules (y-axis) over the test period (x-axis). White areas shows missing data. ....	20
Figure 11: Discrepancy in power output measurements between module S15WhtB4 and the other bifacial modules in the S15Wht array on a clear day, suggesting a measurement rather than performance error. ....	21
Figure 12: Monofacial power (left plots), bifacial power (center plots), and instantaneous bifacial gain (right plots) plotted as a function of solar azimuth (x-axis) and solar elevation (y-axis) for W90 modules. The curved black lines intersecting the colored regions show hours of solar time (e.g., the vertical line labeled 12 is solar noon). The colorbar labels for the bifacial gain plots are the 10 <sup>th</sup> percentile, the 50 <sup>th</sup> percentile (i.e., the median), and 90 <sup>th</sup> percentile bifacial gains. ....	22
Figure 13: Photograph of W90 modules, looking west. Modules W90M1 (left) and W90B2 (right) are visible, while modules W90B1 (far left) and W90M2 (far right) are out of the picture. The power pole that casts a shadow on the W90 modules when the sun is near a west azimuth can be seen directly behind module W90B2. ....	23
Figure 14: Average power output over all days in the six month test period (left), and average instantaneous bifacial gain for the same period (right), plotted as a function of solar time. In the left plots, colors indicate different modules, solid lines indicate bifacial modules, and dashed lines indicate monofacial modules. For example, the yellow dashed line in the top plot is S15WhtM3. In the right plots, colors indicate different pairs of modules used to compute bifacial	

gain. For example, the purple line in the top plot is the bifacial gain calculated from S15WhtB4 and S15WhtM4 using Equation 1.....	24
Figure 15: Average power output over all days in the six month test period (left), and average instantaneous bifacial gain for the same period (right), plotted as a function of solar time. This is a repeat of Figure 14, but condensed to two plots to allow for direct comparison between orientations. To condense, this figure shows the average power and $BGi$ for each module type (bifacial/monofacial) and orientation pair. For example, the solid blue S15WhtB line in the left plot is the average of the four S15WhtB modules. ....	25
Figure 16: Normalized power output for bifacial (blue lines) and monofacial modules (red lines), and instantaneous bifacial gain (black lines) on a cloudy day and a clear day. ....	26
Figure 17: Average bifacial gain during clear periods (solid bars) and cloudy periods (dotted bars) for each of the five array orientations. ....	27
Figure 18: Average daily power output (left), and average monthly bifacial gain in energy (right), plotted by month. In the left plots, colors indicate different modules, solid lines indicate bifacial modules, and dashed lines indicate monofacial modules. In the right plots, colors indicate different pairs of modules used to compute bifacial gain. ....	28
Figure 19: Energy produced by each module (top) – expressed as kWh per $kW_p$ . ( $kW_p = P_{mp}$ ) and the total bifacial gain in energy (bottom) per module for the six-month test period. ....	30
Figure 20: Modeled bifacial gain (Equation 4) in annual energy ( $BGE$ ) for 15° and 30° tilted modules.....	31

## TABLES

Table 1: Orientation and ground surface of test modules.....	11
Table 2: Predicted and measured bifacial gains in energy. ....	32



## 1. INTRODUCTION

Bifacial photovoltaic (PV) modules present an opportunity for increased energy production, better LCOE and more flexible array configurability over conventional monofacial modules by simultaneously accepting light from both sides of a PV array. Sandia National Laboratories and the DOE PV Regional Test Centers (RTCs) for Solar Technologies<sup>1</sup> are testing several arrays of bifacial PV modules from Prism Solar, a U.S. manufacturer of bifacial PV technologies. This report describes performance based on the first six months of operating history of Prism Solar test arrays installed in Albuquerque. Two other similar test arrays are currently being constructed at RTC sites in Vermont and Nevada and will begin operations by the end of 2016. This report therefore provides data and analysis for the Prism Solar installation at the New Mexico RTC only; performance data for the Prism Solar systems at other RTC sites are forthcoming.

The Prism Solar test array examines several variables that are known to influence the performance of bifacial PV arrays. The test array consists of five separate systems at different configurations that vary tilt, azimuth, and reflective properties of the ground cover (albedo). For each configuration, both bifacial and monofacial modules were installed side-by-side, for a total of 32 modules. Each module is grid connected through a microinverter and a research-grade DC monitoring system measures the current and voltage at the maximum power point for each of the 32 modules.

An important aim of this study is to quantify the additional energy that bifacial PV arrays could generate under different conditions and orientations. To do this, we normalized the performance of each module using the conventional STC power rating, measured from the front side of the module. Then, by comparing bifacial and monofacial performance for each orientation, the bifacial gain is determined and reported.

This report is organized into the following sections: (2) System Design, (3) Baseline Testing, (4) Performance Analysis, and (5) Conclusions.

---

<sup>1</sup> For more information on the RTC program: <https://rtc.sandia.gov>

## 2. SYSTEM DESIGN

### 2.1. Module Orientations

Prism Bi60-343BSTC bifacial modules (270W front side STC rating) were installed at the New Mexico RTC, which is located at Sandia National Laboratories in Albuquerque, NM in February, 2016. The modules were mounted at five different orientations, with two different ground surfaces (natural or white), as described in Table 1 and shown in Figure 1. In tandem with the Prism bifacial modules, Suniva OPT265-60-4-100 monofacial modules (265W front side STC rating) are installed in the same orientation and over the same surface, so that a direct comparison of the performance of each module type can be made. The Prism bifacial modules are made from N-type silicon while the Suniva monofacial modules are made from P-type silicon. Both module types are of similar dimensions.

Table 1: Orientation and ground surface of test modules.

<b>Label</b>	<b>Orientation</b>		<b>Ground Surface</b>
	<b>Tilt</b>	<b>Azimuth</b>	
S15Wht	15°	180° (South)	White gravel
W15Wht	15°	270° (West)	White gravel
S30Nat	30°	180° (South)	Natural
S90	90°	180° (South)	Natural
W90	90°	270° (West)	Natural

Naming conventions for each array orientation start with the azimuth of the modules: either “S” for south or “W” for west. Next, the tilt angle is listed. For the non-vertical modules, the ground surface – either “Wht” for white or “Nat” for natural ground – is also listed in the orientation name. The vertical modules were installed over natural ground, which is composed of a gray gravel material.

The schematic in Figure 1 shows the setup of individual modules at each orientation. For the S15Wht, W15Wht, and S30Nat orientations, four bifacial and four monofacial modules were installed. The four bifacial modules were either the four east-most modules (S15Wht and S30Nat) or the four north most (W15Wht) modules. For the S90 and W90 orientations, two bifacial and two monofacial modules were installed. The modules alternated bifacial-monofacial-bifacial-monofacial, when going west to east (S90) or south to north (W90). Bifacial modules were labeled B1, B2, etc. and monofacial modules were labeled M1, M2, etc., as shown in Figure 1.

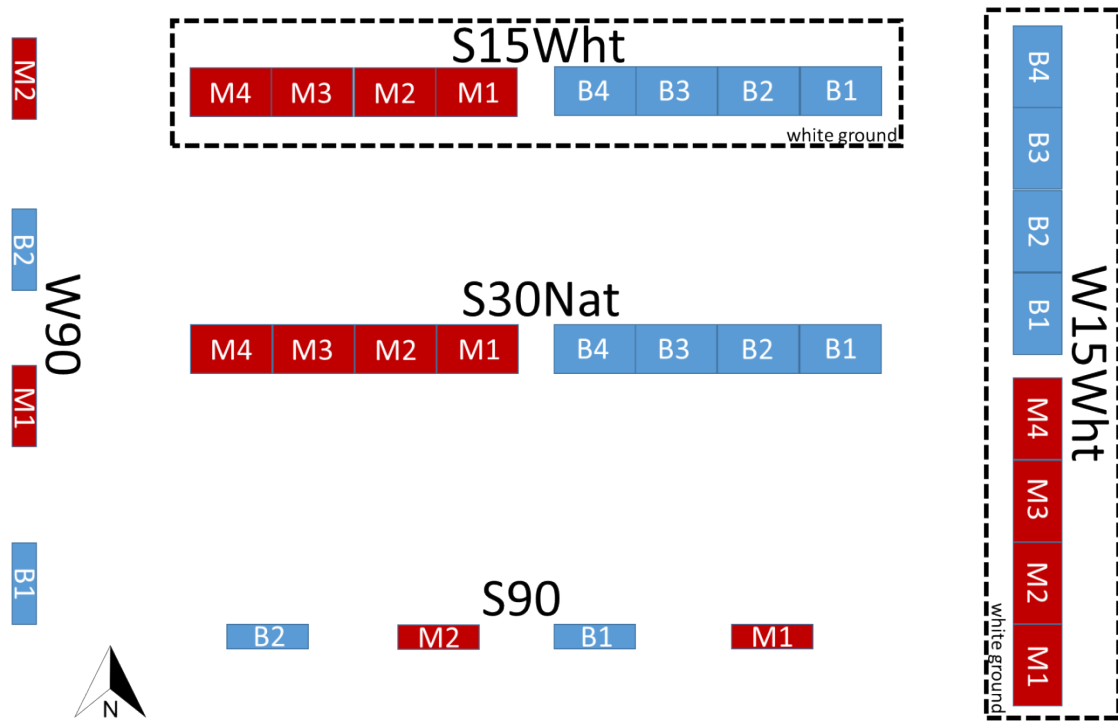


Figure 1: Photograph (top) and schematic (bottom) showing the setup of monofacial and bifacial modules installed at Sandia in Albuquerque, NM. In the schematic, blue represents bifacial modules, red represents monofacial modules, and the two dashed black rectangles indicate the area of crushed white rock that makes up the white ground surface.

## 2.2. Data Acquisition System (DAQ)

Sandia designed a custom monitoring system for the Prism installation to measure the DC output of each module, the temperatures of half the modules, and the front and rear irradiance for each of the five orientations. The instrumentation and data collected are described here:

### DC Electrical – module level

- The DC voltage generated by each module is measured by a resistive divider and is converted to engineering units with an analog to digital converter. This measurement

chain was calibrated and was determined to be accurate to within 0.5% across the full range in voltage and expected field temperature.

b) DC current is measured by an Empro current shunt, and is converted to engineering units with an analog to digital converter. This measurement chain was calibrated and was determined to be accurate to within 0.5% across the full range in current and expected field temperature.

#### AC Electrical – inverter level

Modules are held at their maximum power point by ABB MICRO 0.3-OUTD US microinverters, rated for a maximum usable DC input power of 320W. No inverter clipping was observed. However, once every 15 minutes, these microinverters automatically perform an I-V sweep of the modules in order to ensure they remain at the maximum power point (MPP). This sweep affects every 15<sup>th</sup> 1-minute data point collected by the DAQ system and results in some deviation from MPP for this points.

#### Temperature – module level

Omega thermocouples were installed on half the modules in each array, attaching them at points to minimize shading (Figures 2 and 3). The thermocouple temperature measurements are accurate to within  $\pm 2$  C of true module temperatures. Cell temperatures (not measured) will be several degrees higher than module temperatures.

#### Plane-of-array irradiance – array level

Each array (i.e., each orientation) has two plane-of-array (POA) reference cells from Energy Environmental Technical Services (ETTS): one in the conventional POA of the front of the modules (i.e., front-side irradiance), and a second in the same plane but facing the opposite direction (i.e., back-side irradiance) (see Figure 4.)

All data is measured at two-second intervals and recorded every minute by the system's Campbell Scientific data logger, which averages the data from the preceding minute to record 1-minute resolution timeseries.



Figure 2: Backside of Prism module showing location of yellow thermocouples.



Figure 3: POA reference cell (top center of picture) mounted to measure backside irradiance, shown here for one of the monofacial modules in the W90 orientation. Also visible in the lower right is the yellow thermocouple measuring module temperature.

### 3. BASELINE TESTING

To establish baseline values and meaningful performance comparisons, Sandia ran tests to determine both the ground albedo and the actual maximum power ratings of the modules tested. Measuring the ground surface albedo is important for understanding how much of a performance enhancement is achieved through the more reflective white ground surface. We also conducted flash tests on select modules to determine maximum power ratings and to understand the amount of module-to-module variation, thus allowing for meaningful comparison of bifacial to monofacial power output.

#### 3.1. Ground Surface Albedo

For separate subsets of the six-month test period, Sandia installed an albedometer on either the white or the natural ground surfaces to measure the albedo. The albedometer consists of two CMP-11 pyranometers: one mounted facing the sky measuring global horizontal irradiance (GHI), and the other facing the ground measuring ground reflected irradiance (GRI). The albedo is the ratio of GRI to GHI.

##### 3.1.1. White Ground Surface

The albedometer was installed on the white surface, just east of the W15Wht modules from March 9 - April 5, 2016. A picture of the albedometer and the resultant measurements are shown in Figure 4. Late afternoon shading of the ground surface affected the albedo measurements on all clear and partly cloudy days, as seen in Figure 4. However, apart from shading, the albedo measurements were consistent over both clear and cloudy days: albedo was found to be between 0.5 and 0.6.

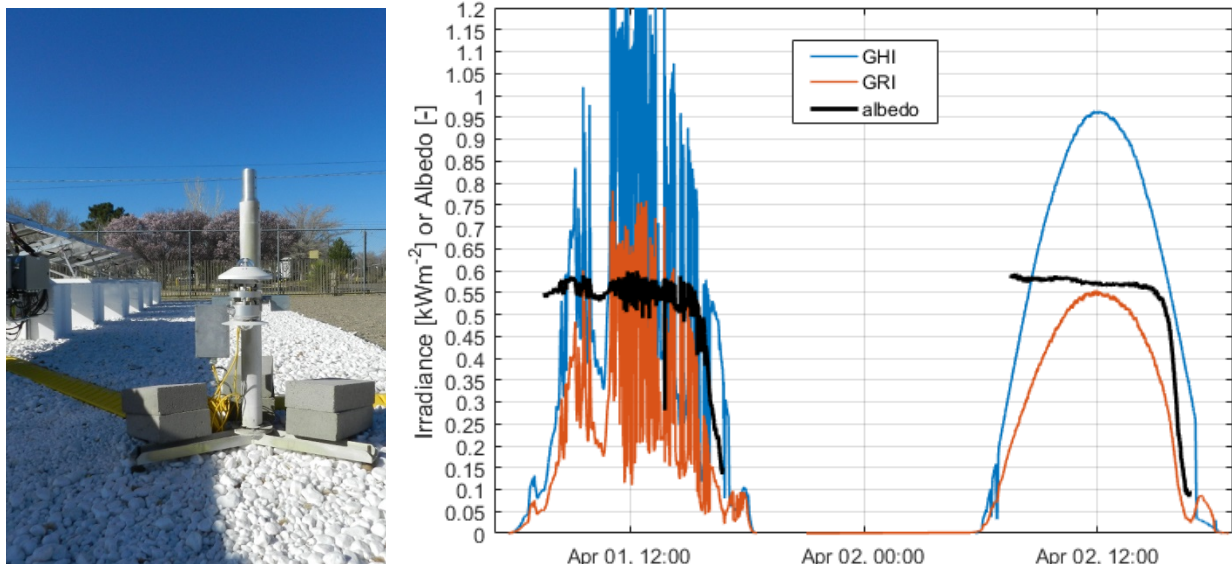


Figure 4: (Left) Albedometer setup on the white surface. The picture was taken in the afternoon, and shows shading of the ground surface. The picture was taken facing north; the albedometer is east of the W15Wht modules. (Right) Global horizontal irradiance (GHI), ground reflected irradiance (GRI), and albedo as measured by the albedometer. Afternoon shading of the ground and hence reduced GRI is visible, especially on the clear day, and is the reason for the reduced albedo in the later afternoon.

### 3.1.2. Natural Ground Surface

After testing on the white ground surface, the albedometer was moved to the natural ground surface. Testing on the natural ground surface lasted from April 20<sup>th</sup> through August 15<sup>th</sup>. The albedometer on the natural surface and GHI, GRI, and albedo measurements are shown in Figure 5. Just as for the white ground surface, albedo measurements were consistent on both clear and cloudy days. The albedo was found to generally be between 0.2 and 0.3.

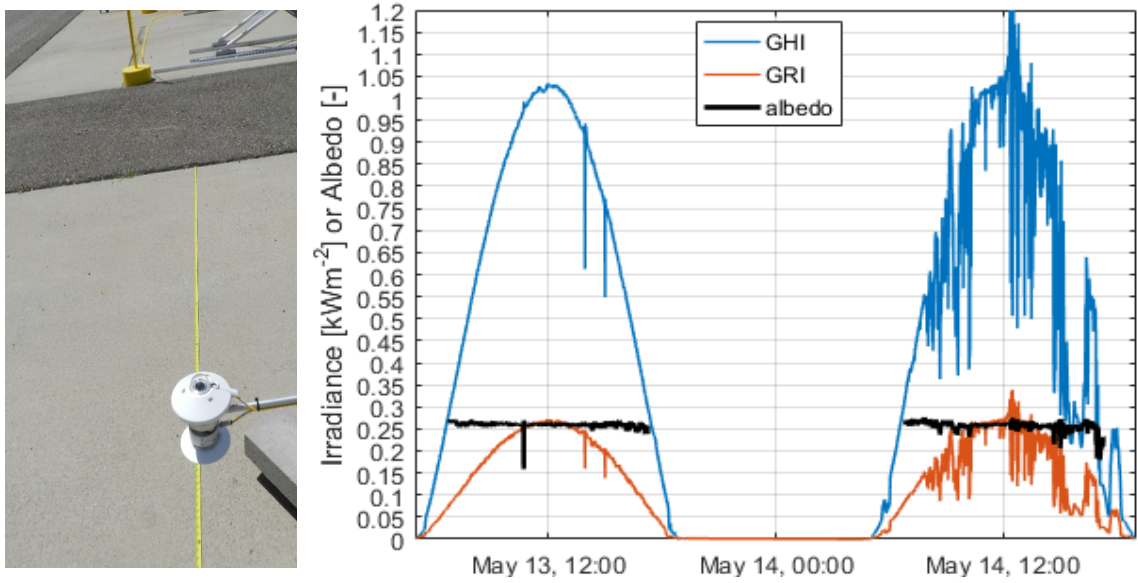


Figure 5: (Left) Albedometer setup on the natural surface. The yellow line is a tap measure used during installation and was not present during albedo measurements. (Right) Global horizontal irradiance (GHI), ground reflected irradiance (GRI), and albedo as measured by the albedometer.

## 3.2. Flash Testing

In July, 2016, after the modules had been in the field for about five months, Sandia selected a sample of ten modules (a monofacial and bifacial module from each of the five array orientations) for flash-testing on Sandia’s Spire 4600 single-long-pulse solar simulator. Bifacial modules were flash tested with the back covered by a black, opaque cloth to block light reaching the backside of the module. The flash-test results give insight into the expected module-to-module variation and allow for comparison of the bifacial to monofacial maximum power ratings on light stabilized modules.

### 3.2.1. Module Front Side Maximum Power

The front side of the Prism bifacial modules has a rated maximum power (P<sub>mp</sub>) of 270W, while the Suniva monofacial modules have a P<sub>mp</sub> rating of 265W; both of these values were determined by the manufacturers at standard test conditions (STC). But, a small variation in P<sub>mp</sub> among modules is to be expected, as some modules are slightly more efficient than others. Specifically, the bifacial modules, which were classified as “test-grade” by their manufacturer, may not have met minimum flash test standards for production modules.

The results of Sandia’s flash tests (Figure 6) show that the Prism modules match their 270W rating with slight (~1%) deviations for two modules. The monofacial modules, however, do not appear to meet their 265W rating, with most modules clustering at approximately 260W P<sub>mp</sub>.

One module has a P<sub>mp</sub> about 1% below 260W. We believe some of this apparent segregation is attributable to Light Induced Degradation (LID), which affects P-type silicon modules such as the Suniva monofacial modules, much more than N-type silicon modules such as the Prism bifacial modules.

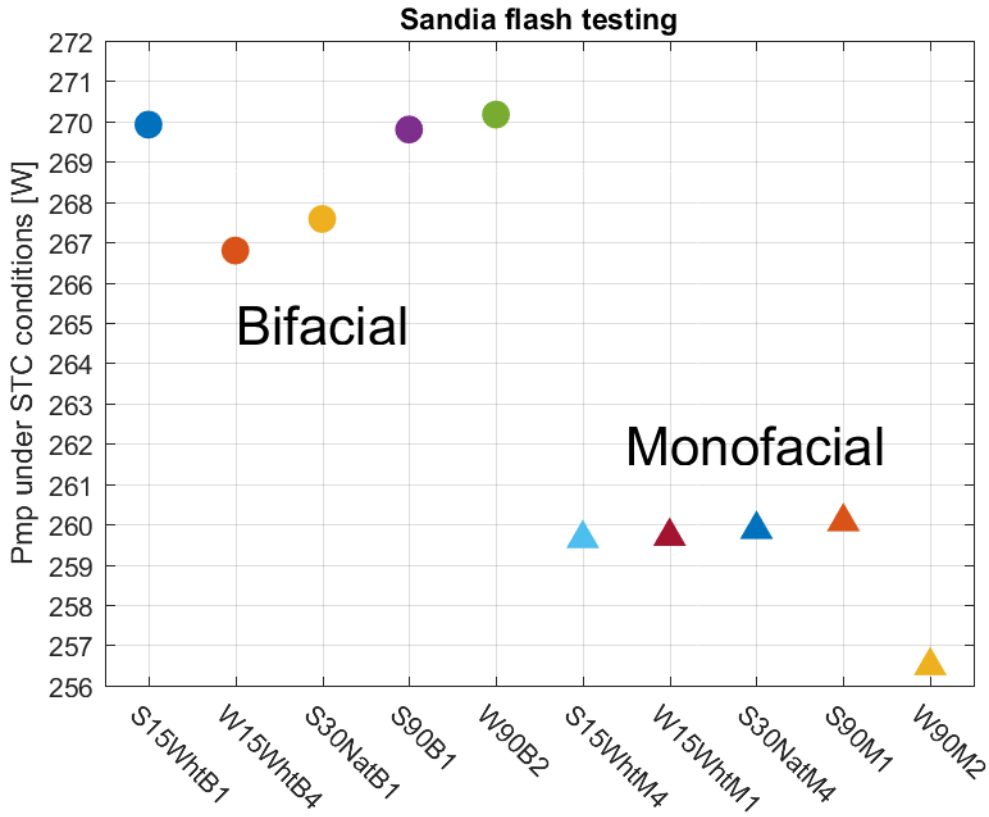


Figure 6: Maximum power (P<sub>mp</sub>) under STC conditions found from front-side flash testing at Sandia.

Additional flash tests (with backside covered) from the Prism Solar factory were made available, and the resultant measured P<sub>mp</sub> values are shown in Figure 7. In general, Prism's flash test results are consistent with the Sandia-performed flash tests in that only a few modules have slight deviations (<1%) from the median. But, the median P<sub>mp</sub> values from the two tests differ by around 2W (~270W for Sandia tests, ~268W for factory tests). This bias may be due to either (a) small systematic differences in flash test procedures and equipment, or (b) slight changes in performance after being sun-exposed for five months. In any case, this difference is less than the typical uncertainty in laboratory flash data.

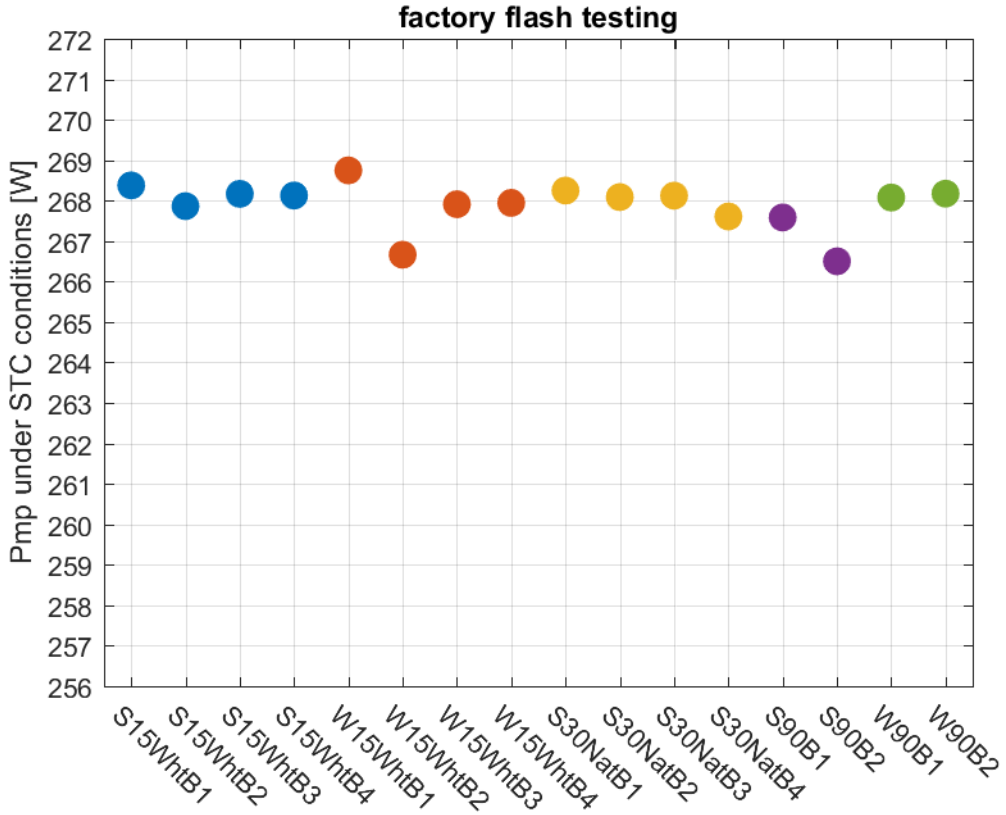


Figure 7: Maximum power (Pmp) under STC conditions found from front-side flash testing at the factory.

Given the uncertainties in flash testing results, and since there are slight module-to-module differences in Pmp values, it would be inappropriate to assign one fixed value for Pmp to all bifacial modules and another fixed value to all monofacial modules. Since not all fielded modules were flash tested, we cannot apply module-specific Pmp values (and even if we did, they would still have some uncertainty due to flash tester uncertainty). Thus, we proceed by assuming a single Pmp value (270W bifacial, 260W monofacial) but note the expected ~3% uncertainty in this measurement. The impact of this uncertainty on performance analysis is mentioned with the analysis in the following sections.

### 3.2.2. I-V Curves

The full I-V curves of the five monofacial modules tested during Sandia flash testing show that all modules had similar responses and consistent short circuit current (Isc) and open circuit voltage (Voc) values, as seen in Figure 8.

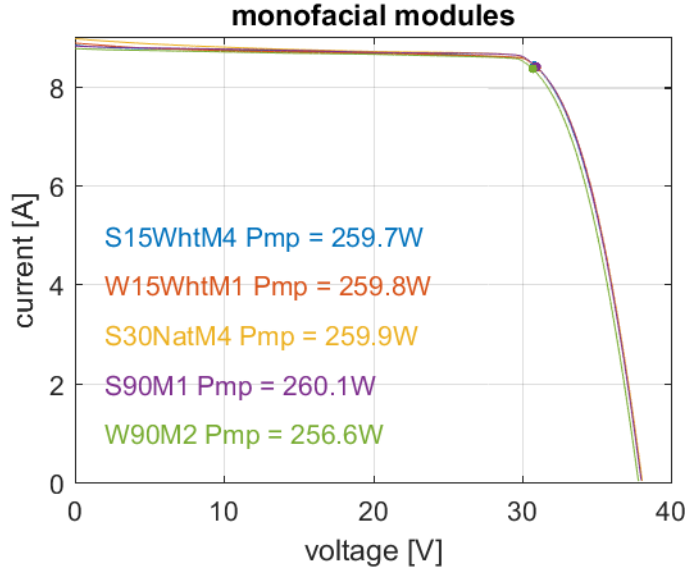


Figure 8: I-V curves for monofacial modules based on flash tests at Sandia.

At Sandia, bifacial modules were flash tested on each side. The back side power ratings are approximately 90% of the front side for the Prism modules (90% ‘bifaciality’). A black, non-reflective cloth was used to cover the side of the module not being tested. The I-V curves confirm that the bifacial modules also perform similarly to one another, as seen in Figure 9. One module (S30NatB1) has a lower backside  $I_{sc}$  than the other modules and has a step in its backside I-V curves, leading to a 7% lower backside  $P_{mp}$  than the average of the other 4 modules. Sandia suspects the lower backside  $P_{mp}$  can be explained by cell-to-cell mismatch affecting the back side of this module. No observable reduction in front side power output was detected from this reduced backside  $P_{mp}$ .

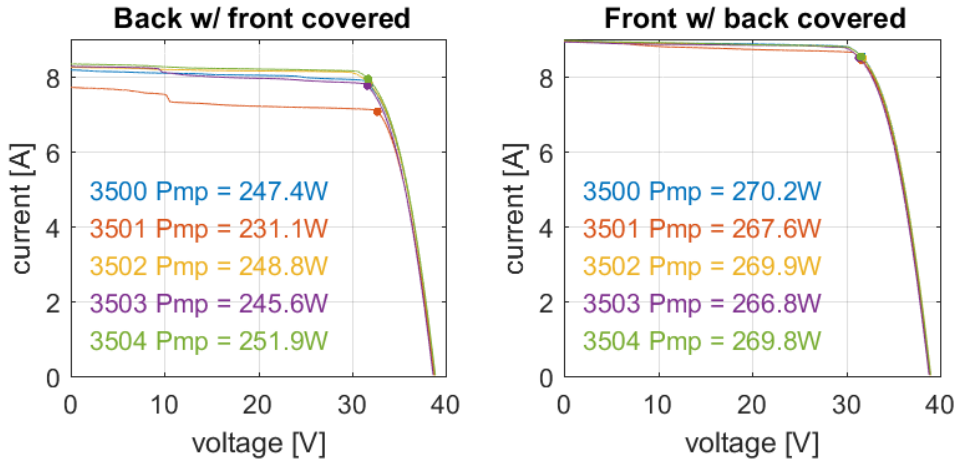


Figure 9: I-V curves for bifacial modules based on flash tests at Sandia.

## 4. PERFORMANCE ANALYSIS

### 4.1. Errant and missing measurements

During the six months of data (February 15 - August 15, 2016) collection described in this report, the arrays functioned well and data was generally available, with three exceptions (Figure 10): on two days in late July, when the system was de-energized to allow for removal of modules for flash testing and then to re-install them; and in late February and early March when module S15WhtM3 experienced technical problems related to its monitoring system.



Figure 10: Data availability for all modules (y-axis) over the test period (x-axis). White areas shows missing data.

Sandia's review of the data shows that module S15WhtB4 had discrepancies in power output from the other three bifacial modules at the same orientation, an effect that appears to have occurred mostly in the July and August measurements (Figure 11). We believe the power discrepancies were caused by problems with the monitoring system because the current measured from module S15WhtB4 was much lower than other modules and occasionally negative during these errant periods, whereas voltages were consistent with other modules. We therefore attribute these power excursions to measurement errors rather than being indicative of actual module performance. We have recently replaced the analog to digital converter on this monitoring system and are investigating the root cause of the deviation.

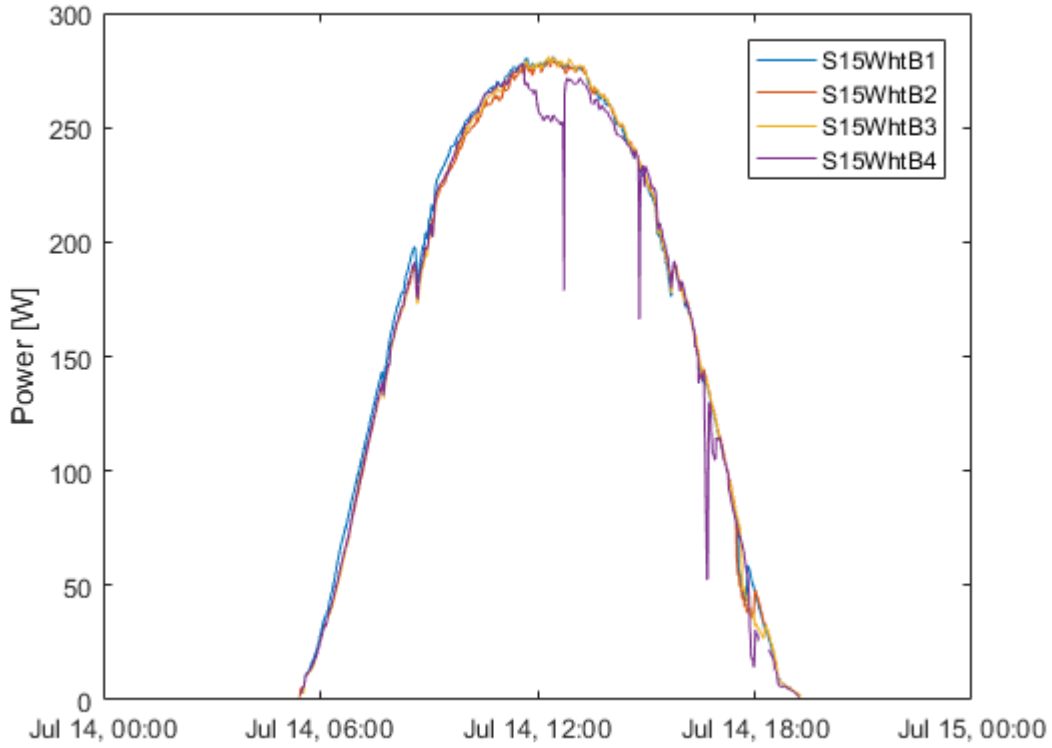


Figure 11: Discrepancy in power output measurements between module S15WhtB4 and the other bifacial modules in the S15Wht array on a clear day, suggesting a measurement rather than performance error.

## 4.2. Performance at Various Sun Angles

The performance difference between bifacial and monofacial modules depends on the incident irradiance on each side of the modules. The gain in energy for the bifacial modules over the monofacial modules thus varies by orientation. We quantify the instantaneous bifacial gain ( ${}^B G_i$ ) as:

$${}^B G_i(t) = 100\% \times \left( \frac{P_{bifacial}(t) / P_{mp\text{bifacial}}}{P_{monofacial}(t) / P_{mp\text{monofacial}}} - 1 \right), \quad 1$$

where  $P_{bifacial}(t)$  and  $P_{monofacial}(t)$  are the bifacial and monofacial power output at time  $t$ , and, based on the flash testing described in section 3.2,  $P_{mp\text{bifacial}} = 270W$  and  $P_{mp\text{monofacial}} = 260W$ . It should also be noted that  $P_{mp}$  values have an expected uncertainty of about 3%, plus the power measurements have additional uncertainty of up to 1% (section 2.2), so there is up to a 4% uncertainty expected in  ${}^B G_i$  values.

### 4.2.1. W90 Modules: Solar Angle Dependent Performance

The W90 modules show the most dramatic differences in power output between monofacial and bifacial modules. For these west-facing modules, direct sunlight is only incident on the front side

for half of the day (afternoon). Figure 12 shows  $P_{\text{monofacial}}$ ,  $P_{\text{bifacial}}$ , and  $BG_i$  for the W90 modules. To show the impact of sun angles, P and BG values are plotted as color intensities, arranged by solar azimuth on the x-axis and solar elevation on the y-axis. Not surprisingly, these plots show that the monofacial modules produce significant power only in the afternoon hours. The bifacial modules, however, produce power in two distinct peaks: once in the morning and once in the afternoon. The bifacial modules produce less power around solar noon, when direct light travels almost parallel to the plane of the modules and so little direct or reflected sunlight is incident on the modules. As expected based on this pattern, the instantaneous bifacial gain is very large in the morning hours:  $BG_i$  can exceed 900%, meaning that bifacial power may be as much as 10x the monofacial power.,  $BG_i$  is smaller around solar noon and in the afternoon hours.

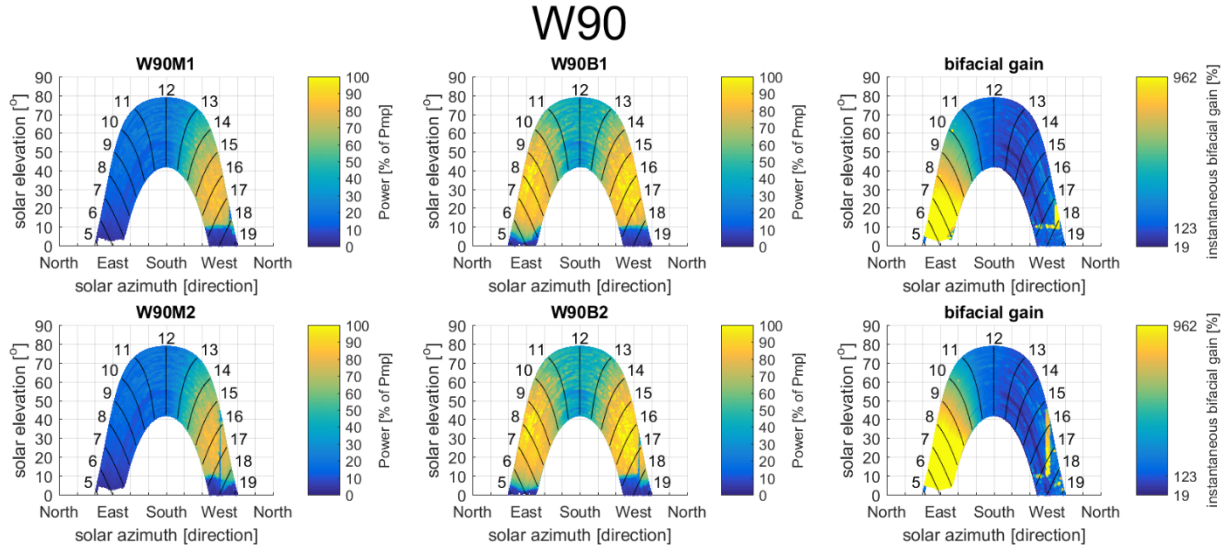


Figure 12: Monofacial power (left plots), bifacial power (center plots), and instantaneous bifacial gain (right plots) plotted as a function of solar azimuth (x-axis) and solar elevation (y-axis) for W90 modules. The curved black lines intersecting the colored regions show hours of solar time (e.g., the vertical line labeled 12 is solar noon). The colorbar labels for the bifacial gain plots are the 10<sup>th</sup> percentile, the 50<sup>th</sup> percentile (i.e., the median), and 90<sup>th</sup> percentile bifacial gains.

Careful examination of the data presented in Figure 12 reveals the impact of shading on performance, especially for the W90M2 and W90B2 modules. When the sun is approximately due west, power output drops significantly, regardless of solar elevation. This anomaly is attributable to a power pole located west of the modules that casts a shadow in the later afternoon (Figure 13). The further north the modules are, the earlier in the day they are shaded by the power pole. This is seen in Figure 12, where W90M2 is shaded earliest, while W90B2 is shaded slightly later in the day. For the southern modules W90B1 and W90M1, the power pole appears further north of west and the impact of shading is less noticeable. Since W90M2 is north of W90B2 and W90M1 is north of W90B1, there is a brief spike in bifacial gain in the afternoon when the monofacial module is shaded but the bifacial module is not. This is most clearly seen in the W90M2/W90B2 bifacial gain plot (bottom right plot in Figure 12).



Figure 13: Photograph of W90 modules, looking west. Modules W90M1 (left) and W90B2 (right) are visible, while modules W90B1 (far left) and W90M2 (far right) are out of the picture. The power pole that casts a shadow on the W90 modules when the sun is near a west azimuth can be seen directly behind module W90B2.

#### 4.2.2. All Modules: Solar Time Dependent Performance

While the W90 modules show the strongest dependence on solar angles for power output, all module orientations are impacted by changing solar angles. Figure 14 shows the power output of the bifacial and monofacial modules and the bifacial gain as a function of solar time for each of the five different orientations. Figure 15 shows the same data (averaged over all modules of the same type and same orientation) on a single plot for cross comparison between orientations. It is important to note that the power output levels over all days in the 6-month period have been averaged: no filtering was applied and therefore both cloudy and clear days and days from all seasons in the six-month period are included in this average. As mentioned in section 2.2, no inverter clipping was observed in any of the modules' power outputs.

For the three south facing arrays (S15Wht, S30Nat, and S90), both bifacial and monofacial modules produce slightly more power in the morning than in the afternoon, largely because of increased module temperatures (and hence lower module efficiency) in the afternoon. Bifacial gains are large in both early morning and late afternoon periods, when the sun may be north of east or north of west and thus direct irradiance is incident on the back of the modules. Larger early morning bifacial gains occur than late afternoon bifacial gains, which is likely an artifact of the installation layout. Because the bifacial modules are installed east of the monofacial modules, the bifacial modules "see" an unshaded ground reflection of irradiance reaching on their backside in the morning, when the modules' shadow is cast off to the west. In the late afternoon, however, as the shadow moves to the east, the bifacial modules are more likely to "see" shaded ground. We also believe that the building to the west of the modules may contribute to late afternoon shading.

The W15Wht modules performance indicates that both bifacial and monofacial modules produced peak power slightly after noon, since they are west-facing. In contrast, the W90 monofacial modules produce peak power well after noon, due to their extreme tilt while the W90 bifacial modules produce more power in the morning than the afternoon, even though their front

(higher P<sub>mp</sub>) side is facing west and back (lower P<sub>mp</sub>) side is facing east. We attribute this discrepancy to higher module temperatures in the afternoon. Overall, the W90 bifacial modules produce significantly more power compared with their monofacial counterparts, which produce very little energy in the morning.

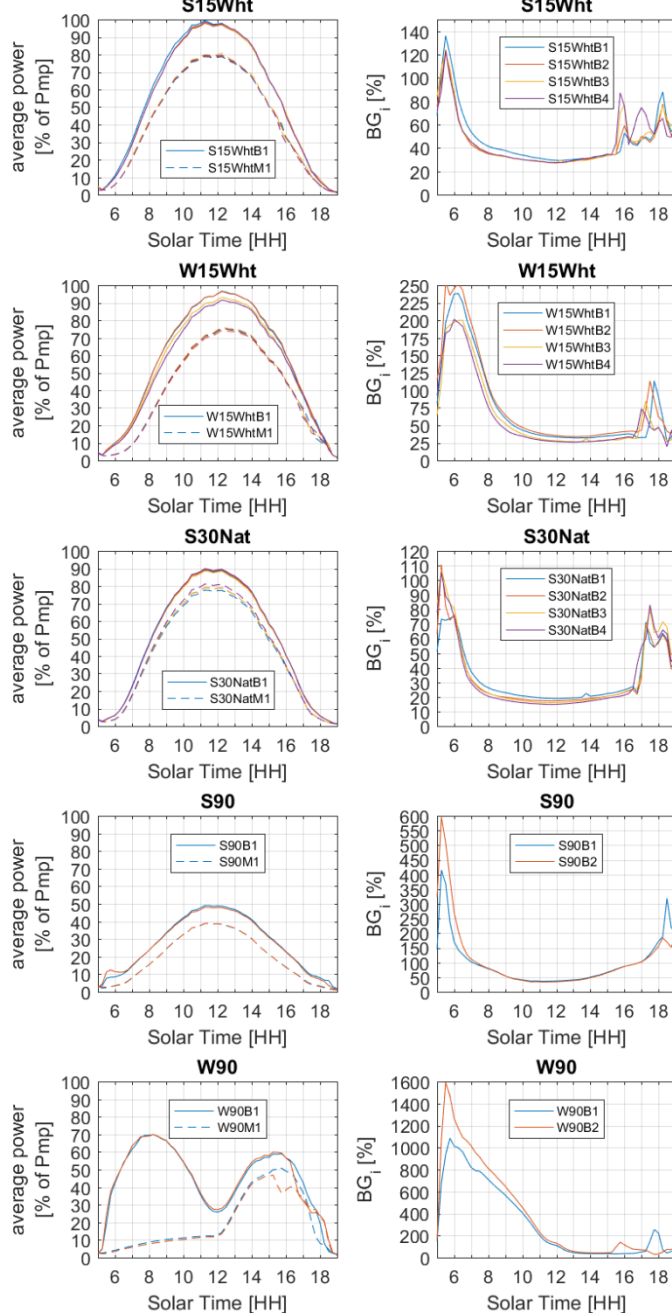


Figure 14: Average power output over all days in the six month test period (left), and average instantaneous bifacial gain for the same period (right), plotted as a function of solar time. In the left plots, colors indicate different modules, solid lines indicate bifacial modules, and dashed lines indicate monofacial modules. For example, the yellow dashed line in the top plot is S15WhtM3. In the right plots, colors indicate different pairs of modules used to compute bifacial gain. For example, the purple line in the top plot is the bifacial gain calculated from S15WhtB4 and S15WhtM4 using Equation 1.

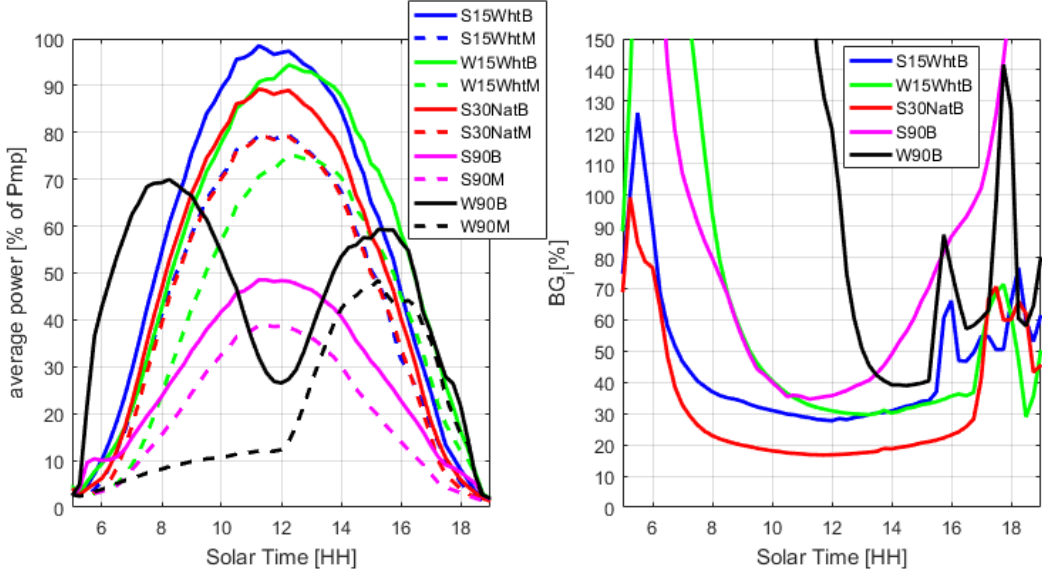


Figure 15: Average power output over all days in the six month test period (left), and average instantaneous bifacial gain for the same period (right), plotted as a function of solar time. This is a repeat of Figure 14, but condensed to two plots to allow for direct comparison between orientations. To condense, this figure shows the average power and  $BG_i$  for each module type (bifacial/monofacial) and orientation pair. For example, the solid blue S15WhtB line in the left plot is the average of the four S15WhtB modules.

### 4.3. Clear vs. Cloudy Conditions

For all the module orientations tested except for W90, the vast majority of irradiance reaching the back side of the modules is diffuse irradiance. This diffuse irradiance comes in two forms: ground reflected diffuse or sky diffuse. Ground reflected diffuse irradiance is often modeled as GHI times albedo and so is larger on clear days (with high GHI) than on cloudy days. Sky diffuse depends on the composition of the atmosphere and is larger on cloudy days when clouds diffuse the irradiance across the sky dome.

To examine the impact of clear and cloudy periods on instantaneous bifacial gains, Figure 16 shows the instantaneous bifacial gains on a cloudy day and a clear day at each orientation. Cloudy periods typically have higher bifacial gains than clear periods. The W90 orientation during morning periods is an exception, as cloudy conditions lead to more generation by the monofacial module since it receives only diffuse irradiance in the morning.

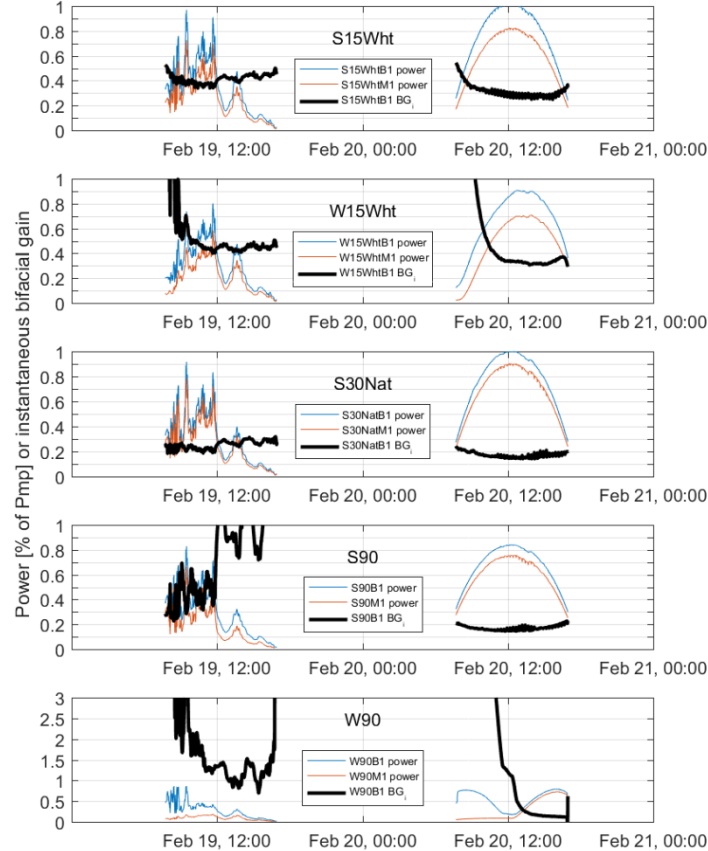


Figure 16: Normalized power output for bifacial (blue lines) and monofacial modules (red lines), and instantaneous bifacial gain (black lines) on a cloudy day and a clear day.

Overall clear versus cloud trends were analyzed by separating clear periods using the detection methods described in [1]. This method identifies clear periods even if they occur on a day that is not fully clear. Approximately 58% of the daytime minutes (when solar elevation  $> 0^\circ$ ) were found to be clear, consistent with the weather conditions in Albuquerque, NM during the test period.

The average bifacial gains during clear and cloudy periods are shown in Figure 17. Differences between clear and cloudy bifacial gains are small for the S15Wht and S30Wht modules. Slightly higher bifacial gain occurs during clear periods for the W15Wht modules because they receive some direct backside irradiance in the morning. S90 modules have higher bifacial gains during cloudy periods, since sky diffuse irradiance is a major part of the irradiance reaching the backside. W90 modules have significantly larger bifacial gains during clear periods, because direct irradiance on the backside in the morning is so important.

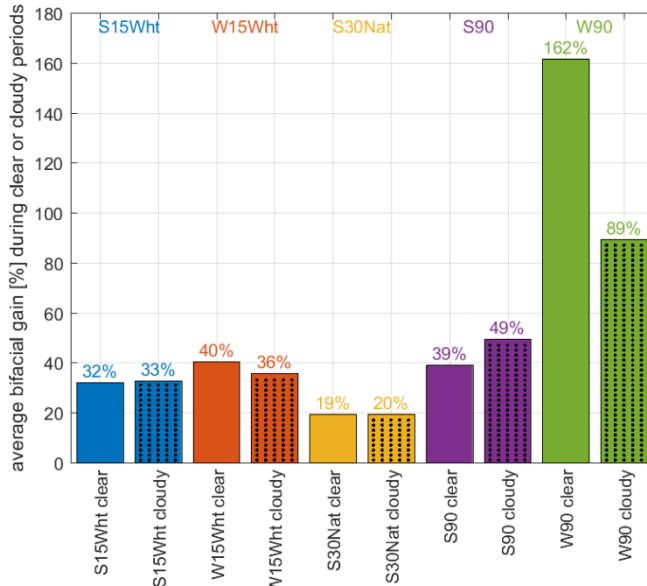


Figure 17: Average bifacial gain during clear periods (solid bars) and cloudy periods (dotted bars) for each of the five array orientations.

#### 4.4. Monthly Bifacial Gains

To explore seasonal trends, we also computed the average energy per day and the monthly bifacial gain in energy ( $BG_E$ ), as shown in Figure 18.  $BG_E$  was computed as:

$$BG_E(1 \text{ month}) = 100\% \times \left( \frac{\sum_{1 \text{ month}} P_{\text{bifacial}} / P_{\text{mp bifacial}}}{\sum_{1 \text{ month}} P_{\text{monofacial}} / P_{\text{mp monofacial}}} - 1 \right) \quad 2$$

We found that all arrays, with the exception of the S90 modules, produced the most energy per day in May, likely due to the combination of high irradiance and cooler temperature conditions than in June, July, or August. In contrast, the S90 modules show a decrease in energy production from February through July due to higher angles of incidence for direct sunlight in summer months than in winter months.

The three south facing arrays (S15Wht, S30Nat, S90) have peak bifacial gains in June, at least partially due to direct irradiance shining on the back of the modules in the early morning and late afternoon. Note that the S15WhtB4 module had artificially reduced bifacial gain in July and August due to the data collection error shown in Figure 11, so these months are not included for this module in Figure 18. Also, while the bifacial gains of the W15Wht modules do not change much seasonally, the W90 modules showed higher bifacial gains in the summer than the winter.

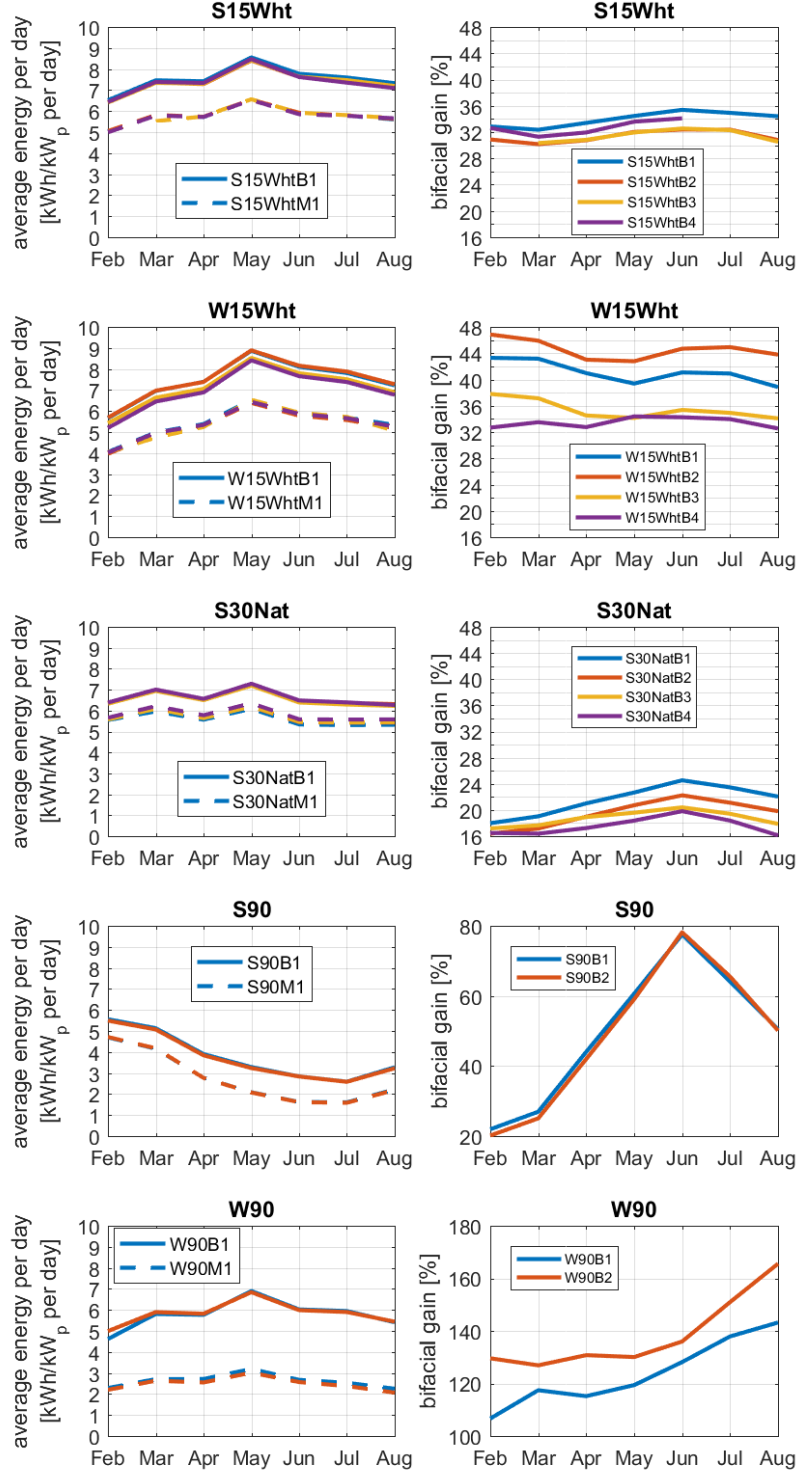


Figure 18: Average daily power output (left), and average monthly bifacial gain in energy (right), plotted by month. In the left plots, colors indicate different modules, solid lines indicate bifacial modules, and dashed lines indicate monofacial modules. In the right plots, colors indicate different pairs of modules used to compute bifacial gain.

## 4.5. Energy and Bifacial Gain over Six Month Period

The total energy produced by each module during the six-month test period is shown in the top plot of Figure 19. The plot has been normalized to show kWh/kW<sub>p</sub>, so that direct comparison can be made between the bifacial and monofacial modules despite their different P<sub>mp</sub> values. Note that kW<sub>p</sub> = P<sub>mp</sub>. From section 3.2, kW<sub>p</sub> is 0.27 kW for bifacial modules and 0.26 kW for monofacial modules. Some variation in total energy among modules of the same type (bifacial or monofacial) and at the same orientation does occur, which may be a result of different shading patterns or deviations in P<sub>mp</sub> ratings (see Figure 7).

As expected, bifacial modules always produced more energy than monofacial modules at the same orientation. It is notable that the W90 bifacial modules produce more energy than monofacial modules at *any* orientation.

The bifacial gains in energy over the six month period,  $BG_E$ , were calculated as follows:

$$BG_E(6 \text{ months}) = 100\% \times \left( \frac{\sum_{6 \text{ months}} P_{\text{bifacial}} / P_{\text{mp,bifacial}}}{\sum_{6 \text{ months}} P_{\text{monofacial}} / P_{\text{mp,monofacial}}} - 1 \right) \quad 3$$

The six month bifacial gains in energy are shown in Figure 19. The W90 modules demonstrate a  $BG_E$  greater than 100%, due to the factors seen in Figure 12, namely the power production in the morning hours when the modules are cooler and hence more efficient. For all other modules, the  $BG_E$  values fall in the 18% to 44% range. The S15Wht and W15Wht modules have higher  $BG_E$  than the S30Nat modules due to the high albedo resulting from the white ground surface, even though the higher tilt of the S30Nat modules leads to more ground reflected irradiance (as more ground surface is “seen” by the module).

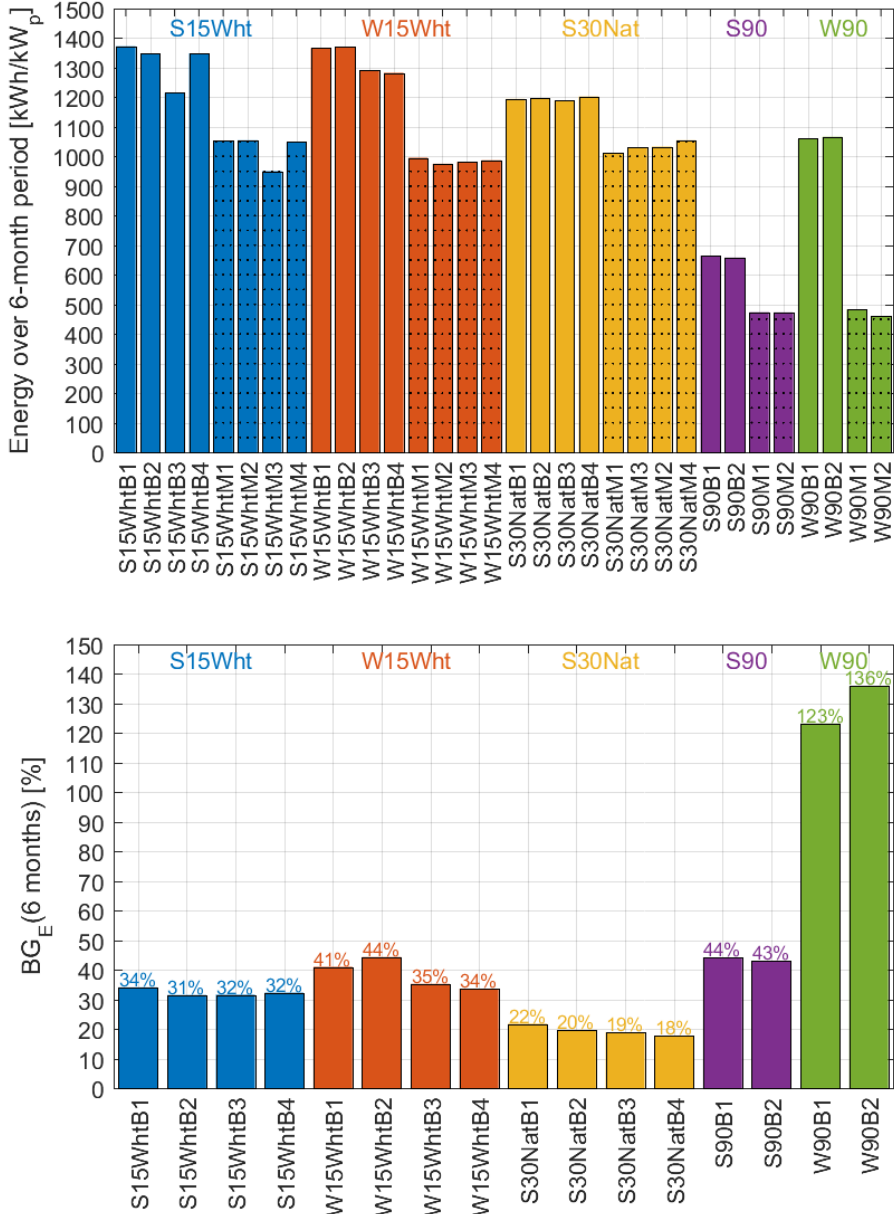


Figure 19: Energy produced by each module (top) – expressed as kWh per kW<sub>p</sub>. (kW<sub>p</sub> = Pmp) and the total bifacial gain in energy (bottom) per module for the six-month test period.

## 4.6. Comparison to Modeled Bifacial Gain

The *Prism Solar Design Guide* [2] suggests Equation 4 to model annual bifacial gain:

$$BG_E(1 \text{ year}) = 0.3 \times \theta + 11.5 \times h + 0.134 \times \alpha, \quad 4$$

where  $\theta$  is the tilt angle of the modules (in °),  $h$  is the height above the ground of the lowest point on the module (in m), and  $\alpha$  is the albedo of the ground surface (in %) and the result is  $BG_E$  in %. This equation is plotted in Figure 20 for both 15° and 30° module tilts. The *Design Guide* suggests that Equation 4 be applied only for module heights that range from 0.15m to 0.8m and

for tilt angles less than  $35^\circ$ . However, for the purposes of this analysis, we apply this equation to the module height range of the RTC tested modules ( $\sim 1\text{m}$ ).

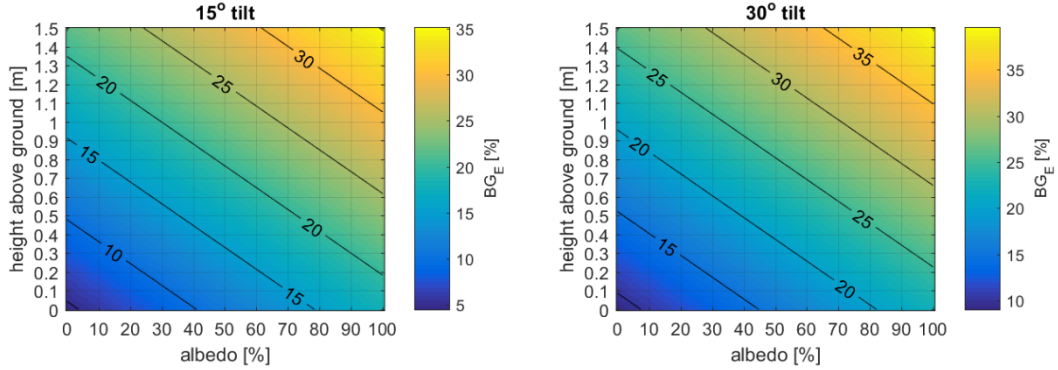


Figure 20: Modeled bifacial gain (Equation 4) in annual energy ( ${}^B G_E$ ) for  $15^\circ$  and  $30^\circ$  tilted modules.

The *Design Guide* also includes an azimuth correction, which is applied to the W15Wht modules: a 162% azimuth correction factor is suggested for a  $90^\circ$  azimuth. For vertical modules, Equation 4 is not recommended. Instead, the *Design Guide* suggests that vertical east-west orientations will yield as much as a 90% bifacial gain.

Table 2 shows the predicted annual bifacial gains in energy (Equation 4) and measured six-month bifacial gains in energy (Figure 19). Since the measured bifacial gains were derived from only six months of data and are not representative of annual solar angle ranges, the measured and predicted bifacial gains are not expected to match exactly. A range of albedo values was used for each bifacial gain prediction, based on the albedo measurements presented in Sections 3.1.1 and 3.1.2.

In most cases, the predicted and measured values were similar. S15Wht modules had slightly higher bifacial gains than predicted, but this may be related to the time of year (mostly summer) when additional irradiance reaches the backside of these modules (when the sun is north of east or north of west). Equation 4 is not meant to apply to tilt angles beyond  $35^\circ$ , yet still closely matches the measured bifacial gains for S90 modules. The measured bifacial gain for the vertical east-west (W90) modules (123% to 136%) was significantly higher than the 90% bifacial gain predicted by the *Design Guide*, which was at least partially due to the backside of the bifacial module facing east and benefitting from cooler morning module temperatures (Figure 14).

Table 2: Predicted and measured bifacial gains in energy.

	Tilt ( $\theta$ )	height (h)	albedo ( $\alpha$ )	azimuth correction factor	Predicted $BG_E(1\ year)$	Measured $BG_E(6\ months)$
S15Wht	15°	1.08m	55-60%		24-25%	34%
						31%
						32%
						32%
W15Wht	15°	1.08m	55-60%	162%	38-40%	41%
						44%
						35%
						34%
S30NatB1	30°	1.03m	20-30%		24-25%	22%
						20%
						19%
						18%
S90	90°	0.89m	20-30%		40-41%	44%
						43%
W90	90°	0.86m	20-30%		~90%	123%
						136%



## 5. CONCLUSIONS

After six months of data collection, Sandia's analysis demonstrates that the bifacial Prism Solar modules are performing well and generating significantly more energy than the reference monofacial modules at the same orientation, even when normalized based on front side STC flash tests. Bifacial gain, which is the additional energy produced by bifacial modules over monofacial modules, was used as the main metric to evaluated the bifacial module performance. Bifacial gains in energy over the six-month test period ranged from 18% to 136% over the five test orientations. These results are consistent with a similar field study run by Prism Solar [3-5].

Several conclusions can be drawn from the data:

First, bifacial gains are not consistent through the day. For south facing modules, power production is largest at solar noon (for both bifacial and monofacial modules), but instantaneous bifacial gains are smallest at solar noon. Bifacial gains are larger in morning and afternoon periods when power output is lower. This suggests that the bifacial gain in energy will be larger than the increased inverter capacity required to capture this energy. For example, the bifacial gain in energy over the six-month period for the S15WhtB1 bifacial module was 35%, while the average instantaneous bifacial gain at solar noon was only 30%. Thus, an inverter only 30% larger could be used to achieve approximately a 35% bifacial gain in energy.

Second, at an off-south pointing orientations (in the northern hemisphere), traditionally considered non-optimal for monofacial systems, energy production of bifacial modules rivals and surpasses that of monofacial modules that are facing south. As bifacial systems deviate from south orientations, the bifacial gain increases, compensating somewhat for the loss of front-side irradiance. For example, west-facing bifacial modules tilted at 15° produced a similar amount of energy as south-facing, 15° tiltedbifacial modules and surpassed the energy production of all the monofacial module orientations considered.

Third, the highest bifacial gain was seen among the vertically tilted bifacial modules, especially those mounted west. In fact, the west-facing, vertically-oriented (i.e., 90° tilted) bifacial modules outperformed monofacial modules at *any* orientation. The drastically different daily power output profile at this west-facing, vertically-oriented orientation (high power in morning and afternoon, low power at solar noon), as compared with more conventional latitude tilt and south azimuth orientations, may be desirable to best match solar power output to electric grid load profiles. While such an orientation is impractical for monofacial modules due to the significant reduction in energy production, it may be feasible for bifacial modules since the loss in energy over more optimal orientations is minor.

Fourth, bifacial gains changed between clear and cloudy conditions. For west facing modules (W15Wht and W90), bifacial gains were higher during clear periods since west-facing bifacial modules benefit from direct irradiance reaching the backside in the morning. South facing modules, on the other hand, had larger bifacial gains during cloudy periods, as the backside receives additional sky diffuse irradiance.

And, fifth, the overall trends in the Prism Solar Model (Equation 4), as specified in previous publications [2-5], have a good correlation with the first six months of data from the New Mexico RTC. In most cases, the measured bifacial gains in energy exceeded those predicted by the Prism Solar Model, although this is likely explained by the module height being slightly outside of the recommended applicability range, and, especially, by the time of year (summer) in the six-month study period, when bifacial gains are expected to be larger due to the greater range in sun azimuth angles (the sun rises north of east and sets north of west in the summer). We expect that the measurements and Prism Solar Model will be in even closer agreement when a full year of data is considered.



## REFERENCES

- [1] M. J. Reno and C. W. Hansen, "Identification of periods of clear sky irradiance in time series of GHI measurements," *Renewable Energy*, vol. 90, pp. 520-531, 2016.
- [2] Prism Solar Technologies Inc. (September 2, 2016). *Prism Solar Design Guide Revision 4.1* Available: [http://www.prismsolar.com/pdf/Design\\_guide.pdf](http://www.prismsolar.com/pdf/Design_guide.pdf)
- [3] J. E. Castillo-Aguilella and P. S. Hauser, "Multi-Variable Bifacial Photovoltaic Module Test Results and Best-Fit Annual Bifacial Energy Yield Model," *IEEE Access*, vol. 4, pp. 498-506, 2016.
- [4] J. E. Castillo-Aguilella and P. S. Hauser, "Bifacial Photovoltaic Module Best-Fit Annual Energy Yield Model with Azimuthal Correction," presented at the Photovoltaics Specialists Conference (PVSC), Portland, OR, 2016.
- [5] J. E. Castillo-Aguilella, "Multi-Year Study of Bifacial Energy Gains Under Various Field Conditions," presented at the 4th PV Performance Modelling Workshop, Cologne, Germany, 2015.



**DISTRIBUTION**

1 MS0899      Technical Library      9536 (electronic copy)



